



# Registration of small (below 1%) changes of calcium ion concentration in aqueous solutions and in serum by the constant potential coulometric method

Anna V. Bondar, Valentina M. Keresten, Konstantin N. Mikhelson\*

Chemistry Institute c/o St.Petersburg State University, 26 Universitetsky Prospect, Stary Peterhof, 198504 St. Petersburg, Russia

## ARTICLE INFO

### Keywords:

Calcium ion activity  
Constant potential coulometry  
High sensitivity  
Blood model solutions  
Serum

## ABSTRACT

Small changes (down to 0.1%) of  $\text{Ca}^{2+}$  ion activity in pure solutions of  $\text{CaCl}_2$ , model solutions mimicking blood serum, and blood serum sample are registered by constant potential coulometric measurements, using solid contact ion-selective electrodes (ISEs) with poly(vinyl chloride) (PVC) membrane containing ETH 1001 as neutral ionophore. A new measurement protocol is proposed aimed at a significant improvement of the signal-to-noise ratio in the current measurements. A procedure is developed for the PEDOT-PSS deposition on glassy carbon from mixed water-acetonitrile solution. Data are obtained in support of Kragh-Hansen and Vorum's approach for the quantification of the interaction between  $\text{Ca}^{2+}$  ions and bovine serum albumin (BSA).

## 1. Introduction

Ion-selective electrodes (ISEs) with sensor membranes containing ionophores, for several decades, are successfully used as potentiometric sensors in various applications. Enormously broad linear working range: up to ten decades in concentration [1,2] together with a constant value of the resolution of the measurements make the potentiometry with ISEs advantageous in comparison with many other analytical techniques. On the other hand, in the potentiometric measurements the resolution, being constant over the whole response range, is, per se, too high for many applications. This resolution is directly proportional to the charge value of the analyte ion, and therefore measurements with high resolution are especially challenging in the case of divalent ions e.g.  $\text{Ca}^{2+}$ . The constant potential coulometry method invented in the Bobacka's group addresses this issue [3–5]. This method allows for a drastic improvement of the sensitivity of the measurements [6]. Initially, this method was verified with  $\text{K}^+$ -selective SC ISEs as a model system [3–6]. Later the constant potential coulometry was applied successfully for the assay of divalent ions [7] and anions [8]. The quantitative theory of the current and charge response considers the electrode as a resistor (sensor membrane) connected with a capacitor (a conducting polymer (CP) layer) in series [9]. The modified theory also considers the concentration polarization in the membrane caused by the current flow [10].

It is tempting to use the peak current as the analytically relevant

signal because its value is large and therefore promising for a high sensitivity and resolution. However, the procedure of changing the solution composition takes time resulting in an ambiguity about the  $t_0$  value. At longer values of time the uncertainty about the  $t_0$  is less important, however the current value is well below the peak. Also, the modification of the composition of the sample requires stirring, and the latter makes the signal noisy. On the contrary, the charge value obtained by integration of the current over time is low sensitive to the uncertainty about  $t_0$ , and less noisy because of integration. It is especially important that the charge value is proportional to the capacitance of the CP [5,9,10]. Relatively large capacitance value is the reason for higher resolution of the constant potential coulometry over potentiometry.

Unfortunately, obtaining a steady value of charge requires long time. In our group it was proposed to cut off the measurements, and it was shown that both current and charge recorded at a certain time are linearly dependent on the logarithm of the activity of the target ion. This allows plotting calibration graphs for further interpretation of the measurements in samples [10].

Another approach aimed at reducing the response time in the constant potential coulometry was proposed by the Bakker's group [11]. The use of an electronic capacitor in series with the electrode allows for a significant decrease of the time needed for the saturation of charge. Furthermore, the electronic capacitor may play the same role as the CP layer, so the constant potential coulometry can be implemented also

\* Corresponding author.

E-mail addresses: [konst@km3241.spb.edu](mailto:konst@km3241.spb.edu), [k.mikhelson@spbu.ru](mailto:k.mikhelson@spbu.ru) (K.N. Mikhelson).

<https://doi.org/10.1016/j.snb.2021.131231>

Received 31 August 2021; Received in revised form 6 December 2021; Accepted 7 December 2021

Available online 13 December 2021

0925-4005/© 2021 Elsevier B.V. All rights reserved.

with classical ISEs with internal aqueous solution [12,13].

In this work we have modified the protocol of the measurements in the constant potential coulometry mode. The new protocol allowed for a significant improvement of the signal-to-noise ratio. The study was performed with  $\text{Ca}^{2+}$  SC ISEs as a model system because a precise control of  $\text{Ca}^{2+}$  is especially important in the clinical diagnostics [14–16]. For the first time, we used  $\text{Ca}^{2+}$  sensor in the constant potential coulometry mode in blood model solutions with a constant ionic strength, and in blood serum, and achieved 0.1% resolution in the measurements of  $\text{Ca}^{2+}$  ion concentration in these complex matrices. Like it was shown elsewhere [13], we confirm that in the case of small additions it is useful to plot the signal against concentration (not logarithm) of the analyte. Additionally, we describe here a simplified procedure for obtaining the CP layer on the surface of the glassy carbon.

## 2. Experimental

### 2.1. Chemicals and materials

Calcium ionophore I diethyl N,N'-[(4R,5R)-4,5-dimethyl-1,8-dioxo-3,6-dioxaoctamethylene] bis(12-methylaminododecanoate)] (ETH 1001), cation-exchanger potassium tetrakis(p-Cl-phenyl)borate (KCITPB), lipophilic electrolyte tetradodecyl ammonium tetrakis(p-Cl-phenyl)borate (ETH 500), plasticizer 2-nitrophenyl ether (oNPOE) were from Merck (Germany), ethylenedioxythiophene (EDOT) was from Fluorochem (UK) and sodium polystyrene sulfonate (NaPSS) was from Aldrich (USA). High molecular weight poly(vinyl chloride) (PVC) was from Ohtalen (Russia). Tetrahydrofuran (THF) was from Vekton, and distilled before use. Inorganic salts (analytical grade) were from Reaktiv (Russia). Bovine serum albumin (BSA) was from Dia.M (Russia). 2-[4-(2-hydroxyethyl)piperazin-1-yl]ethanesulfonic acid (HEPES) was from Carl Roth (Germany). Serum samples uTroll Control serum were from Thermo Scientific (Finland). Model solutions mimicking serum were prepared by dissolving suitable amounts of inorganic salts, BSA and HEPES in DI water. After that the pH of the solutions was adjusted at 7.35 by small additions of NaOH. All aqueous solutions were prepared with deionized (DI) water with resistivity of 18.2 M $\Omega$ ·cm (Milli-Q Reference, Millipore).

The membrane cocktail contained PVC (460 mg), oNPOE (920 mg), ETH 1001 (14.3 mg), KCITPB (4.5 mg), ETH 500 (21.0 mg) in 7.8 mL of THF. The mixture was gently mixed for 30 min using roller-mixer Selecta Movil Rod (Spain).

### 2.2. Electrode preparation

Glassy carbon electrodes representing glassy carbon rods (GC) with diameter of 3 mm, in Teflon bodies with outer diameter of 7 mm were from Volta (Russia). Prior to deposition of the CP layer, the electrodes were modified as follows. Plasticized PVC tubes with a diameter of 8 mm were soaked in acetone for 1 day. As a result, the tubes became swollen, while the plasticizer was extracted to acetone. The electrodes were placed into swollen tubes and let for the acetone evaporation. During the evaporation of acetone, the tubes shrunk tightly on the Teflon bodies, forming outer PVC coating, as shown in Fig. S1 (Supporting Information). After that, the surfaces of glassy carbon rods were thoroughly polished on shabby leather with diamond slurry P/N 250.1030 on P/N 259.1025 substrate from Antec Scientific (The Netherlands) and then with 0.3 mm alumina paste from Buehler (USA). Then the electrodes were rinsed with DI water, placed into 1 M  $\text{HNO}_3$  for 5 min, rinsed with DI water and sonicated in ethanol for 5 min (Elmasonic L15H, Elma). Finally, the electrodes were sonicated for another 5 min in DI water.

The polyethylenedioxythiophene (PEDOT) layer on the surface of GC electrodes was formed by galvanostatic electropolymerization as described in detail in Section 3.1.

The membranes were formed by drop-casting of 70  $\mu\text{L}$  of the membrane cocktail on the top of the electrode, in two equal consecutive

drops. The cocktail covered the whole surface: PEDOT + Teflon + PVC coating. The direct contact of the membrane layer with the PVC outer coating helped to prevent delamination of the membranes from the electrodes.

### 2.3. Measurements

Zero-current potentiometric measurements were performed with 8-channel potentiometric station Ecotest 120 (Econix, Russia). Electropolymerization procedure and non-zero current measurements were carried out with potentiostat-galvanostat Autolab 302 N (Metrohm, Switzerland). The reference electrode in all measurements was Ag/AgCl in saturated KCl, with a custom-made flexible low-leak salt bridge filled with the same solution. The counter electrode in the non-zero current measurements was bare glassy carbon rod. Automatic sequential dilution of samples was done with 700 Dosino / 711 Liquino system (Metrohm, Switzerland).

The measurements were performed in the potentiometric mode and in the chronoamperometric mode. The coulometric signal was obtained by integration of the chronoamperometric curve. The measurements in pure  $\text{CaCl}_2$  were performed either using sequential 10-fold dilution of the initial 0.1 M  $\text{CaCl}_2$ , or by additions of suitable aliquots of  $\text{CaCl}_2$  to initial 0.1 mM  $\text{CaCl}_2$  solution. In model solutions the ISEs were calibrated in the potentiometric mode, while for the chronoamperometric/coulometric measurements suitable aliquots of  $\text{CaCl}_2$  were added to model solution with 1 mM  $\text{CaCl}_2$ . When working with serum samples, the ISE potential was registered in the zero-current mode in an unaltered sample, and then a current was recorded along with small additions of  $\text{CaCl}_2$ .

In all measurements we used 10 mL samples. The choice of this volume values is explained below. If the sample initially contains 1 mM  $\text{Ca}^{2+}$ , a change of this value in 0.1% means adding 1  $\mu\text{M}$  of  $\text{CaCl}_2$ . Use of stock solutions with high concentrations, e.g. 1 M, requires addition of volumes below 1  $\mu\text{L}$ , which we avoided. Use of diluted stock solutions results in significant increase of the sample volume, so small amounts of  $\text{CaCl}_2$  do not cause increase of the concentration of the analyte. For small changes we therefore used 10 mM  $\text{CaCl}_2$  as stock solution, and made additions of 1 or a few microliters to 10 mL samples.

The pH measurements were carried out with a glass pH electrode ESL-43–07 (Izmeritel, Belarus). All measurements were performed with 3 replicate electrodes.

For the improvement of the signal-to-noise ratio, the procedure of the chronoamperometric measurements was modified as described in Section 3.3.

## 3. Results and discussion

### 3.1. Modification of the technique of the deposition of PEDOT-PSS layer on glassy carbon

Normally, PEDOT-PSS layer is deposited on a substrate electrochemically, most often galvanostatically, from aqueous solution containing EDOT and NaPSS [17–20]. The polymerization stage, per se, takes a few minutes. However, the preparation of a solution of EDOT in water takes several hours, with a continuous stirring to obtain a clear solution. This makes the whole procedure of the deposition of PEDOT-PSS layer on a substrate time-consuming. Organic solvents (e.g. acetonitrile) or mixed aqueous-organic solvents (water/methanol) are also used in the polymerization of EDOT [21,22]. We therefore explored a new procedure which, to the best of our knowledge, has never been used before. It is known that EDOT and NaPSS readily dissolve, respectively, in acetonitrile and in water. We therefore prepared two separate solutions: 0.1 M EDOT in acetonitrile and 0.1 M NaPSS in water. Then we mixed 1 mL of EDOT in acetonitrile with 9 mL of NaPSS in water, immediately obtaining a clear solution ready for the polymerization.

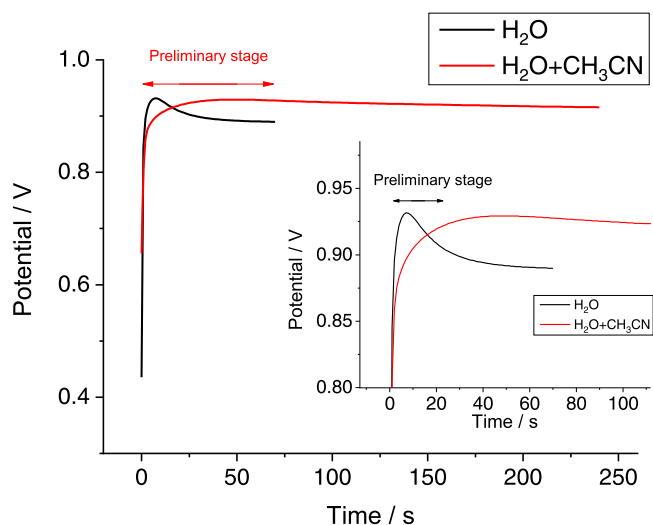


**Fig. 1.** Chronopotentiometric curves of the galvanostatic deposition of PEDOT-PSS layer on glassy carbon electrodes from aqueous (black line) and mixed aqueous-organic (red line) solutions of EDOT and NaPSS. The inset shows the initial part of the deposition procedure.

The PEDOT-PSS layer on the surface of GC was formed galvanostatically, by passing current with the density of  $0.2 \text{ mA/cm}^2$ . Initially, the current was passed for 70 s as suggested earlier for glassy carbon rods with the diameter of 3 mm [5]. However, it turned out that this time is not enough for the formation of the PEDOT-PSS film from mixed aqueous-organic solution. We therefore tried other time protocols: 240, 480 and 720 s, and it turned out that 240 s was enough to obtain the film. The polymerization curves recorded in aqueous and mixed aqueous-organic solutions are presented in Fig. 1. Both curves contain a maximum in the initial part of the curve. This maximum is typical for galvanostatic electropolymerization of EDOT-PSS and may be ascribed to the formation of oligomers of EDOT or to the initial nucleation of the polymer species at the glassy carbon surface (a preliminary stage of the process). The width of this maximum was ca. 20 s when we used aqueous solution, and ca. 70 s in the case of mixed water-acetonitrile solution. Apparently, the preliminary stage of the formation of the PEDOT-PSS film on glassy carbon in mixed aqueous-organic solution requires more time than in water.

The polymerization charge was calculated assuming the initial stage did not contribute to the polymer film formation, so the time value used in the calculations was 170 s. The estimated charge was therefore 2.4

mC, and the estimated film thickness was  $0.5 \mu\text{m}$ . The capacitance of the film was estimated by the impedance measurements. The results are presented in Figs. S2, S3 (Supplementary Material). The shape of the spectrum was typical for a capacitive behavior and the estimated capacitance value was  $9.2 \cdot 10^{-5} \text{ F}$ .

### 3.2. Control of the quality of the ISEs

Prior to chronoamperometric/coulometric measurements, the ISE response to  $\text{Ca}^{2+}$  in pure  $\text{CaCl}_2$  and in model solutions was controlled by the EMF measurements. Calcium ion activity coefficients in pure and in mixed solutions were calculated by the Davies equation (the 3rd approximation of the Debye-Hückel theory), using 6 as the Kielland parameter for  $\text{Ca}^{2+}$  [23]. The results are presented in Fig. S4 (Supporting Information).

### 3.3. Modification of the chronoamperometric measurements procedure

The measurements with ISEs in the constant potential coulometry mode suggest integration of the recorded current to obtain the cumulated charge. Integration largely suppresses noise, therefore the charge curve is much smoother than the current curve, as indicated elsewhere [6]. The most attractive feature of the constant potential coulometry mode of the measurements with ISEs is the enhanced sensitivity to small changes in the concentration of the analyte. Small changes of the concentration result in small currents, and the current signal becomes increasingly noisy [6]. Therefore, it is desirable to improve the signal-to-noise ratio in the chronoamperometric measurements. The noise is produced primarily by stirring. On the other hand, stirring is necessary to make the sample uniform after it is diluted or spiked with an addition. To circumvent this problem, we modified the measurements procedure as described below and shown in Fig. 2A.

In the modified procedure of the measurements, immediately before any modification of the composition of the sample the cell is turned off. When the sample composition is modified, e.g., the sample is diluted, or an addition is spiked, the stirrer is turned on for 20 s. Experiments with dyes showed that this time is far enough to make the resulting composition of the sample solution uniform. After that the stirrer is turned off and then the cell is turned on.

As shown in Fig. 2B, such a modification allows obtaining significantly smoother curve than the ordinary mode with the stirrer continuously on. Data shown in the right inset clearly show that in the end of the current curve, in the ordinary mode of measurements the noise prevails and implies the current is constant:  $I = (-4.6 \pm 3.0) \cdot 10^{-9} \text{ A}$ . On the contrary, the modified mode reveals that current is still regularly

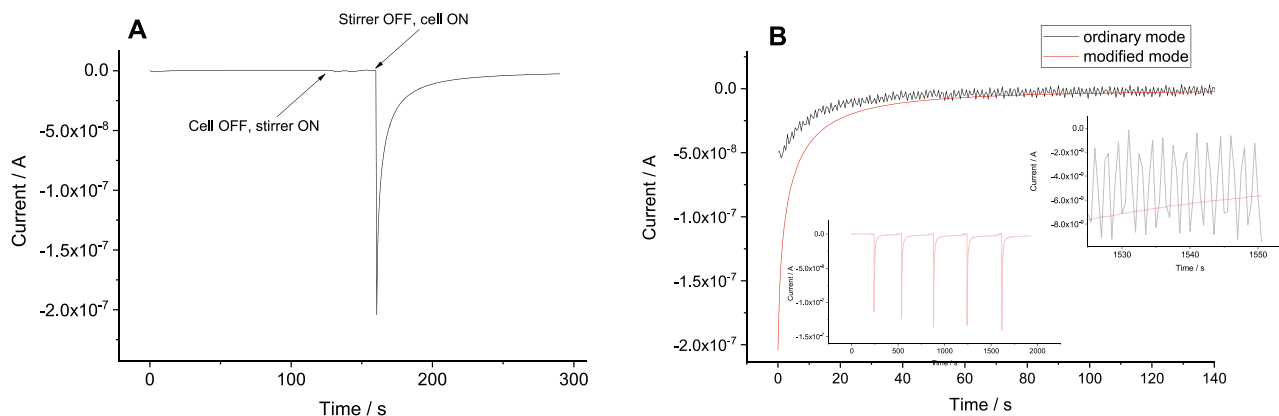


**Fig. 2.** A: scheme of the modified measurements procedure. B: Comparison of the current curves recorded using the ordinary and the modified procedures of the measurements. The data refer to the change of the  $\text{CaCl}_2$  concentration from 0.25 to 0.50 mM. The inset in the left part of the figure refers to sequential two-fold increase of the concentration of  $\text{CaCl}_2$ : from 0.25 mM to 0.50 mM, to 1 mM, to 2 mM, to 4 mM, and finally to 8 mM. The inset in the right part refers to the end of the current curve.

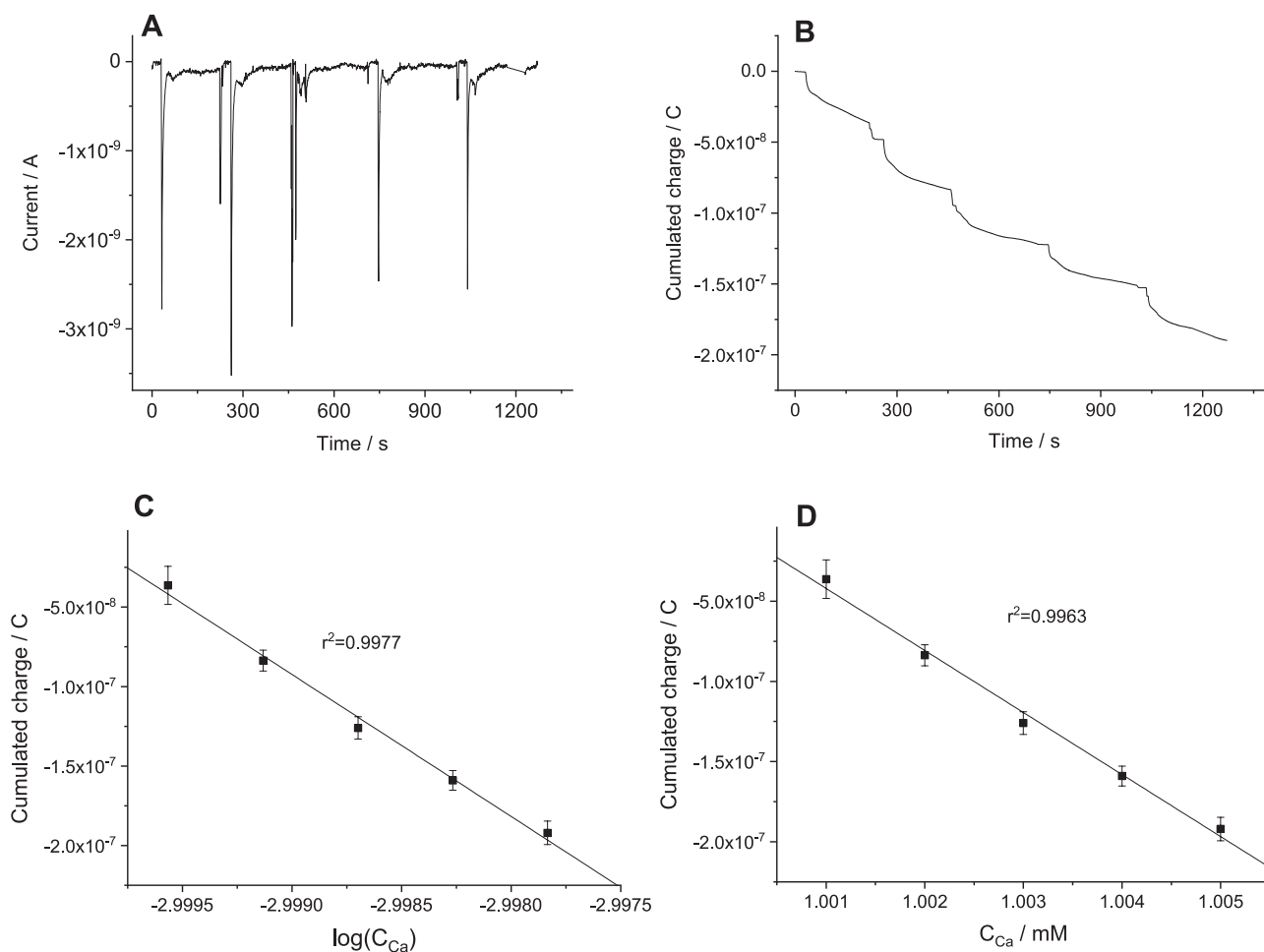


**Fig. 3.** Additions of pure  $\text{CaCl}_2$  to 1 mM  $\text{CaCl}_2$ . A: current caused by five sequential additions of 0.001 mM to the initial 1 mM  $\text{CaCl}_2$ . B: the respective charge curve (integration of the current curve). C: cumulated charge (100 s after addition) plotted vs. logarithm of the molar concentration of  $\text{CaCl}_2$ . D: cumulated charge plotted vs. the concentration of  $\text{CaCl}_2$  in mM.

changing. Even if the data are treated as a constant value, the respective result is  $I = (-6.45 \pm 0.17) \cdot 10^{-9}$  A, thus the SD is 50 times lower. Also, the current peak is sharper, and a larger initial current is registered.

### 3.4. Sensitivity to small additions of $\text{CaCl}_2$

The main advantage of the constant potential coulometry with ISEs over the potentiometric readout is the significant improvement of the sensitivity. Therefore, we focused our further study on small additions of  $\text{CaCl}_2$  to (i) pure solutions of  $\text{CaCl}_2$  in water, to (ii) blood model solutions containing inorganic salts and glucose, to (iii) blood model solutions containing also BSA, and to (iv) blood serum samples.

#### 3.4.1. Pure solutions of $\text{CaCl}_2$

The total concentration of calcium in blood serum varies from 2.10 to 2.55 mM, while the ionized calcium ( $\text{Ca}^{2+}$ ) makes roughly one half of the total value and varies from 1.16 to 1.32 mM [14]. Therefore, for measurements in pure aqueous media we have chosen 1 mM  $\text{CaCl}_2$  as the initial solution. Next, by adding suitable aliquots of 10 mM  $\text{CaCl}_2$  the  $\text{Ca}^{2+}$  concentration in the sample increased to 1.005 mM, in five sequential steps, 0.001 mM each. Thus, in each step the  $\text{Ca}^{2+}$  concentration increased by 0.1%. The results are presented in Fig. 3. The current curve (see Fig. 3A) is very much noisier than that shown in Fig. 2B. This is because the results shown in Fig. 2B refer to two-fold additions which caused currents in the range of  $10^{-7}$  A, whereas 0.1%- additions resulted in currents in the range of  $10^{-9}$  A. The charge curve (Fig. 3B) is

much smoother because charge is obtained by integration of current over time.

The values of charge cumulated after the sequential additions are plotted vs.  $\log(C_{\text{Ca}})$ : the logarithm of the  $\text{Ca}^{2+}$  molar concentration (Fig. 3 C) and vs.  $C_{\text{Ca}}$  (Fig. 3 D). Ideally, equal changes in the  $\text{Ca}^{2+}$  ion concentration must result in equal values of the cumulated charge. The error bars in the calibration graphs are calculated as standard deviations of the values obtained in individual measurements from the respective mean value. The sensitivity to small concentration changes is excellent: the concentration of  $\text{Ca}^{2+}$  ions ( $C_{\text{Ca}}$ ) increased from 1 mM to 1.005 mM, i.e. the whole range of  $\log(C_{\text{Ca}})$  is only 0.0174 logarithmic units, and in  $C_{\text{Ca}}$  the whole variation is within 0.5%. Since the overall change of the concentration (and of the ionic strength) was so small, plotting against logarithm of the concentration (not the activity) is justified, and the obtained linearity is very encouraging. From the practical point of view, it is especially important that the cumulated charge linearly depends also on the analyte concentration (not the logarithm). This is because the additions are small in comparison with the initial value of the  $\text{Ca}^{2+}$  concentration, and therefore the approximation  $\log\left(\frac{f_0}{f_0}(1+x)\right) \approx x$  is valid, like it was shown for  $\text{Na}^+$  measurements by the Bakker's group [13].

#### 3.4.2. Model solutions without albumin

$\text{Ca}^{2+}$ -ISE, as well as other ISEs with ionophore-based membranes are widely used in clinical analyzers for the measurements of blood electrolytes, and it is known that ISEs normally deliver reliable data [15].

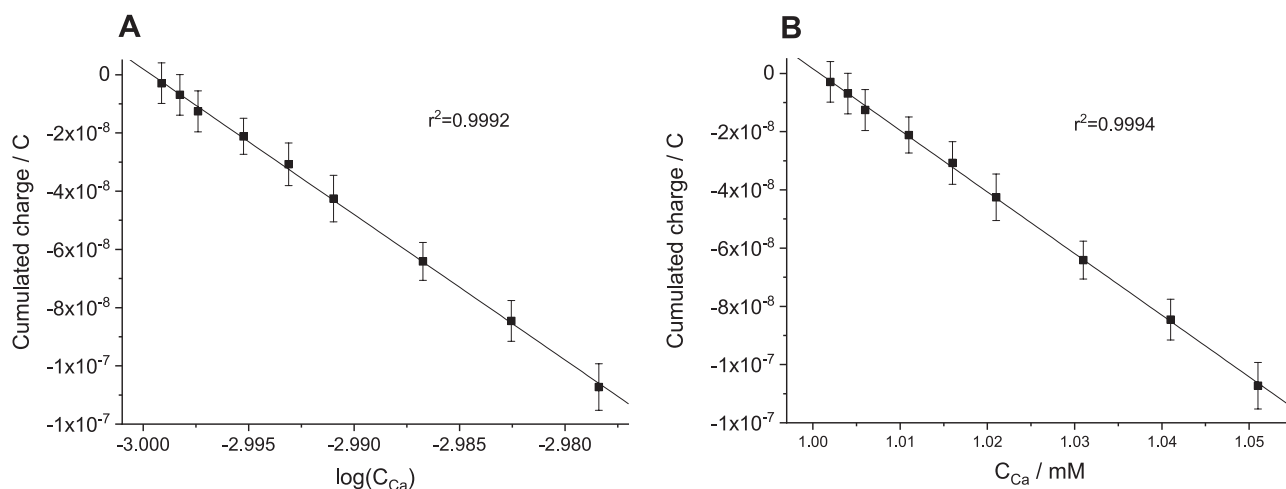


**Fig. 4.** Cumulated charge (100 s after addition) obtained after sequential additions of pure  $\text{CaCl}_2$  to model solution with 1 mM  $\text{CaCl}_2$ . A: cumulated charge plotted vs. logarithm of the molar concentration of  $\text{CaCl}_2$ . B: cumulated charge plotted vs. the concentration of  $\text{CaCl}_2$  (mM).

However, in clinical analyzers the ISEs are in contact with serum samples for a relatively short time, and in between the samples the ISEs are in contact with calibrator solutions and, from time to time, also with washing solutions. This allows for minimizing of biofouling of the ISE membranes caused by the adsorption of proteins at the ISE membrane surface [15]. In the constant potential coulometric measurements the ISEs may be in contact with the sample for a longer time, so biofouling could deteriorate the response. Therefore, in this study we used two kinds of model solutions mimicking blood serum: without proteins, and with bovine serum albumin (BSA). This was done to reveal whether a prolonged contact with albumin is critical for the ISE response.

The basic model solution contained 100.0 mM NaCl, 34.0 mM  $\text{NaHCO}_3$ , 4.0 mM KCl, 0.5 mM  $\text{MgCl}_2$ , 5.5 mM Glucose, 5.5 mM Urea and also HEPES, 12 g/L. HEPES is often used for the pH stabilization in solutions containing calcium [1,14]. The initial pH of the basic solution was 6.8, and the final value pH 7.35 was adjusted by adding small amounts of NaOH, under a continuous potentiometric control of the pH with a glass pH electrode.

Aliquots of  $\text{CaCl}_2$  producing  $\text{Ca}^{2+}$  concentrations from 0.25 to 8 mM were added to the basic solution immediately before the measurements. The potentiometric response of the ISEs in the model solutions (together with that in pure solutions of  $\text{CaCl}_2$ ) is shown in Fig. S4 (Supporting Information). One can see that the potentials recorded in model solutions are consistent with those recorded in pure solutions of  $\text{CaCl}_2$ : the EMF values recorded in the two kinds of solutions belong to the same straight line with the slope 30.2 mV/log( $a_{\text{Ca}}$ ). Only at the lowest concentration of  $\text{CaCl}_2$  (0.25 mM) in model solution the potential slightly deviates from the Nernstian response, obviously, due to the interference from  $\text{Na}^+$  and other cations.

Chronoamperometric/coulometric measurements in model solutions were carried out in the same way as in pure aqueous  $\text{CaCl}_2$ . The initial concentration of  $\text{Ca}^{2+}$  was 1 mM. Then it was increased to 1.006 mM (in three steps, 0.2% each), next to 1.021 mM (in three steps, 0.5% each), and finally to 1.051 mM (in three steps, 1% each). The recorded current curve and charge curve are shown in Fig. S5 (Supporting Information), and the respective calibration curves are presented in Fig. 4 A, B. One can see that the linearity in both plots is excellent, and it is possible to detect the change of  $\text{Ca}^{2+}$  concentration of 0.2%.

### 3.4.3. Model solutions with bovine serum albumin

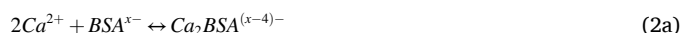
In real blood and serum samples calcium is largely complexed by albumin, other proteins and phosphates. For the interpretation of the data obtained for calcium different quantities are discussed. The so-called “corrected ionized calcium” refers to value obtained at an actual pH and corrected to pH 7.4 [16]. The so-called “albumin adjusted

total calcium” refers to value obtained at an actual concentration of albumin and corrected to albumin concentration of 37 g/L [23–28]. The ratio of the ionized calcium concentration over the total calcium is ca. 45–55% [29–31], although the correlation between these two values is sometimes poor [32].

Since albumin is present in real serum and blood, it appears reasonable to add it to model solutions used in studies of sensors. To prepare these solutions BSA was added to the basic model solution (pH 7.35) in concentrations 10, 20, 30, 40 and 50 g/L. Given the molar ratio of BSA is 66,500, the respective values of the total concentration of BSA were 0.150, 0.301, 0.451, 0.602 and 0.752 mM. Therefore, unlike in solutions without BSA, the activity of  $\text{Ca}^{2+}$  ions cannot be calculated directly using the value of the total concentration of calcium and the ionic strength of the solution. A correction must be made for the complexation of  $\text{Ca}^{2+}$  with BSA. This correction can be introduced in different ways. It is possible to consider a number of equilibria involving  $\text{Ca}^{2+}$  ion and different binding sites in a protein (e.g. albumin), so that the interaction of  $\text{Ca}^{2+}$  ion with each of the sites is described by a specific association constant, also known as Scatchard binding constants [33–35]. A simplified approach [34] considers only two association equilibria:



$$K_1 = [\text{CaBSA}^{(x-2)-}] / (a_{\text{Ca}} \cdot [\text{BSA}^{x-}]) \quad (1b)$$



$$K_2 = [\text{Ca}_2\text{BSA}^{(x-4)-}] / (a_{\text{Ca}}^2 \cdot [\text{BSA}^{x-}]) \quad (2b)$$

Kragh-Hansen and Vorum [34] performed dialysis experiments using cells divided into two equal compartments by a cellulose membrane. Initially, one compartment contained calcium salt, albumin, and a pH buffer, whereas the other compartment contained the buffer only. Free  $\text{Ca}^{2+}$  ions were able to penetrate the membrane, and the equilibrium content of the total calcium in both compartments was measured using radio tracers ( $^{45}\text{Ca}$ ). In this way it was shown that at pH 7.40 the aforementioned equilibrium constants are  $K_1 = 1513$  and  $K_2 = 647$ .

We have measured  $a_{\text{Ca}}$ : the activity of  $\text{Ca}^{2+}$  ions in model solutions containing different concentrations of BSA using our ISEs in the potentiometric mode, the results are presented in Fig. S4 (Supporting Material). After measurements, the ISEs reproduced the calibration in pure  $\text{CaCl}_2$  solutions. We therefore ascribe the changes in the ISE potentials to decrease in the  $\text{Ca}^{2+}$  concentration due to complexation with albumin.



**Table 1**

Concentrations of  $\text{Ca}^{2+}$  ions (measured), free BSA (calculated with Eq. (3)), and the total calcium (calculated as  $[\text{Ca}]^{\text{tot}} = [\text{Ca}^{2+}] + [\text{CaBSA}] + [\text{Ca}_2\text{BSA}]$ ) in model solutions with constant  $[\text{Ca}]^{\text{tot}} = 2.00$  mM and different concentrations of total BSA.

Total BSA		$[\text{Ca}^{2+}]$ , mM	[BSA], mM	$[\text{Ca}]^{\text{tot}}$ , mM
g/L	mM			
10	0.150	$1.98 \pm 0.01$	0.038	$2.10 \pm 0.02$
20	0.301	$1.81 \pm 0.01$	0.080	$2.03 \pm 0.02$
30	0.451	$1.66 \pm 0.02$	0.128	$1.98 \pm 0.03$
40	0.602	$1.56 \pm 0.02$	0.179	$1.98 \pm 0.03$
50	0.752	$1.43 \pm 0.03$	0.237	$1.95 \pm 0.05$

The data on the activity of free  $\text{Ca}^{2+}$  ions allow for calculation of the concentration of free BSA in solution with a known total content of BSA:

$$[\text{BSA}] = [\text{BSA}^{\text{tot}}] / (1 + a_{\text{Ca}} \cdot K_1 + a_{\text{Ca}}^2 \cdot K_2) \quad (3)$$

Once  $a_{\text{Ca}}$  is measured and the concentrations of CaBSA and  $\text{Ca}_2\text{BSA}$  are calculated using  $K_1$ ,  $K_2$  and  $C_{\text{BSA}}$ , one can obtain the total concentration of calcium, and in this way estimate the reliability of the calculations. Our results obtained for the total  $C_{\text{Ca}}^{\text{tot}} = 2.0$  mM and different values of the total concentrations of BSA are presented in Table 1.

One can see that the calculated value of the total concentration of calcium is rather close to the target value of 2 mM, suggesting reliability of the estimations made. We therefore used values  $K_1 = 1513$  and  $K_2 = 647$  for calculations of the concentrations of free  $\text{Ca}^{2+}$  ions when aliquots of  $\text{CaCl}_2$  were added to model solutions with 40 g/L total BSA. Within the range of  $[\text{Ca}]^{\text{tot}}$  from 1 mM to 1.05 mM the calculated value of the fraction of ionized calcium was practically constant:  $[\text{Ca}^{2+}] / [\text{Ca}]^{\text{tot}} \approx 0.7868$ . Thus, the relative changes of the total concentration of calcium and those of the ionized calcium are the same, e.g., an addition of 0.1% total calcium results in 0.1% increase of ionized calcium, etc.

The results of the measurements of the effect of small additions of  $\text{CaCl}_2$  to model solutions containing 40 g/L BSA (i.e., 0.602 mM total BSA) are presented in Figs. 5 and S5 (Supporting Information). One can see that 0.1% change in calcium content in model solutions containing BSA can be detected.

#### 3.4.4. Measurements in serum samples

Thermo uTroll Control serum samples were used in this study. Potentiometric measurements with 3 replicate  $\text{Ca}^{2+}$ -ISEs showed that the ionized calcium concentration in samples was ca. 1 mM. Aliquots of 10 mM  $\text{CaCl}_2$  (always 1  $\mu\text{L}$ ) were sequentially added to 10 mL serum sample. The original current/time curves and the respective cumulated

charge curves are presented in Figs. S8, S9 (Supporting Information). Due to tiny values of currents, the current curves are noisy, especially in the case of ISE 1, see Fig. S8. Furthermore, noise caused by the manipulations when additions were spiked resulted in noise in the charge curve so that the charge signal was not always monotonous, see Fig. S9. Therefore, the results obtained in serum samples are shown here as follows. For each of the ISEs, currents recorded once the cell is on after each of the additions are plotted together, see Figs. 6 and S10. This representation allows for better visualization of the current peaks and of their reproducibility in between sequential additions.

Charge values cumulated in the course of sequential additions are shown in the analogous way, see Figs. 7 and S11.

Charge values cumulated by 100 s after additions were used to plot calibration graphs shown in Figs. 8 and S12. Ideally, the charge curves should coincide. The error bars in the calibration graphs are calculated as standard deviations of the values obtained in individual curves from the mean value. High values of the correlation coefficients ( $r^2 \geq 0.999$ ) indicate good linearity of the calibration graphs. Like in Sections 3.4.1.–3.4.3., the linearity vs. the concentration changes (not logarithms) is because the additions are small in comparison with the initial value of the  $\text{Ca}^{2+}$  concentration. It is also important that the extrapolation of the graphs to zero addition results in a virtually zero charge value.

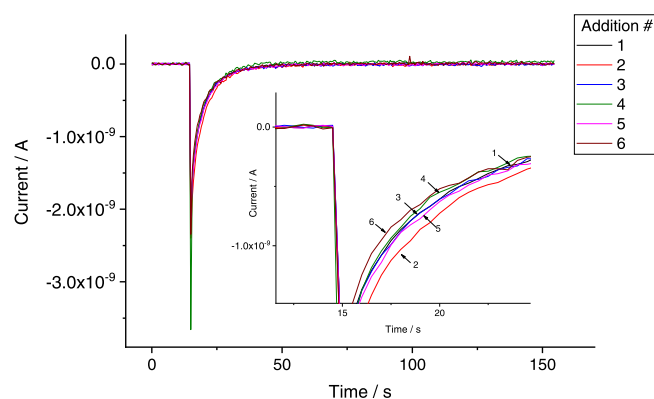


**Fig. 6.** Currents recorded with ISE 1 after sequential 0.1% additions of  $\text{CaCl}_2$  to serum sample.

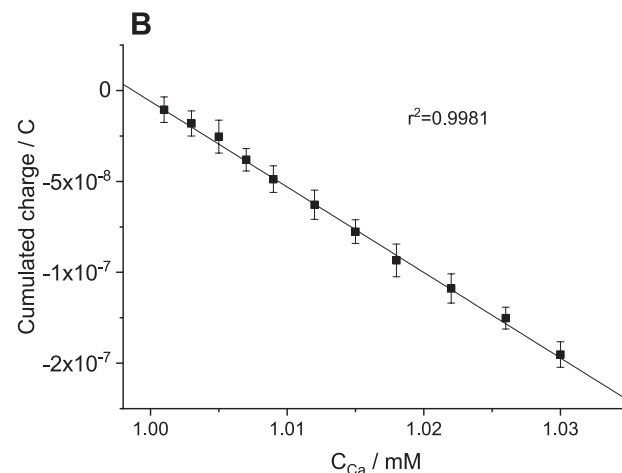
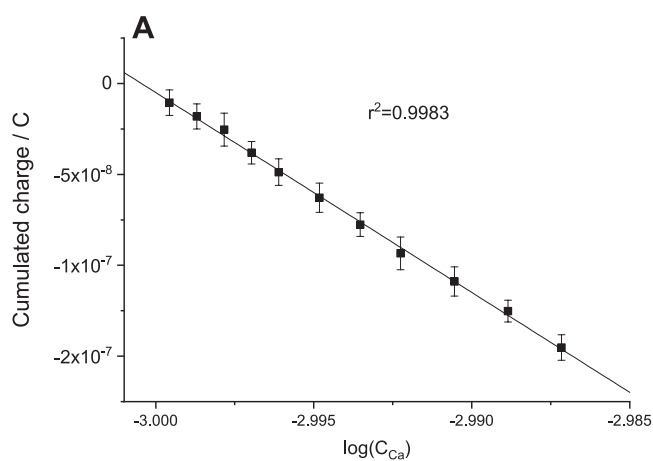


**Fig. 5.** Cumulated charge (100 s after addition) obtained after sequential additions of pure  $\text{CaCl}_2$  to model solution with 40 g/L total BSA and 1 mM  $\text{CaCl}_2$ : 0.1%, 0.2% (three times), 0.3% (three times), 0.4% (three times) and 0.5%. A: the cumulated charge plotted vs. logarithm of the molar concentration of  $\text{CaCl}_2$ . B: the cumulated charge plotted vs. the concentration of  $\text{CaCl}_2$  in mM.

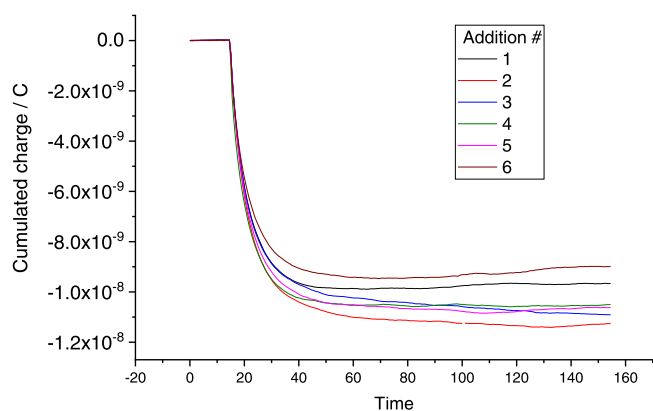


Fig. 7. Charge values obtained using ISE 1 after sequential 0.1% additions of  $\text{CaCl}_2$  to serum sample.

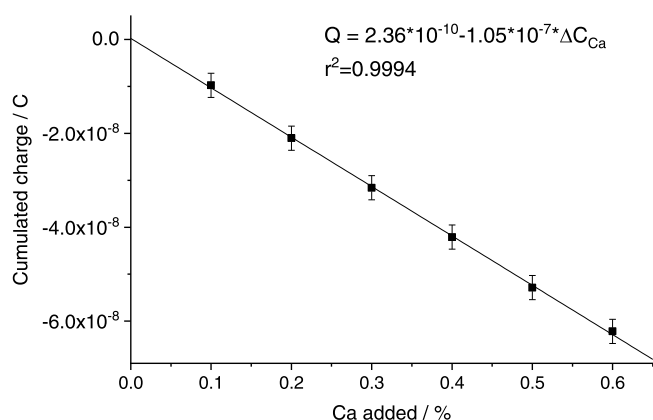


Fig. 8. Calibration graph obtained with charge values cumulated by 100 s after additions of  $\text{CaCl}_2$  to serum sample, ISE 1.

#### 4. Conclusions

This study confirms new opportunities offered by the constant potential coulometry method for detection of small changes of the composition of samples. With  $\text{Ca}^{2+}$ -ISEs as model system, a concentration changes of  $1 \mu\text{M}$  at a concentration level of  $1 \text{ mM}$ , i.e., a 0.1% change in the  $\text{Ca}^{2+}$  ion activity, were detected in pure solutions of  $\text{CaCl}_2$ , as well as in solutions mimicking blood serum, and in Thermo uTroll control serum samples.

For the chronoamperometric measurements a novel protocol is proposed which allows for a significant decrease of the electrostatic noise. The protocol is especially useful in the case of small differences in the analyte concentrations in samples since the respective currents are rather small and otherwise prone to electrostatic interferences [6].

The interaction of  $\text{Ca}^{2+}$  with BSA is studied in the potentiometric mode, and it is shown that the simple approach proposed by Kragh-Hansen and Vorum [34] can be utilized for the calculation of free (ionized) calcium content in solutions with known total calcium and total BSA concentrations.

A convenient procedure is developed for a galvanostatic deposition of PEDOT-PSS films on glassy carbon surface.

#### Funding

The study was supported by the Russian Foundation for Basic Research, Project 19-03-00259.

#### CRediT authorship contribution statement

AB: experimental work and discussion, VK: experimental work and discussion, KM: Conceptualization, discussion, writing.

#### Declaration of Competing Interest

The authors declare that they have no known competing financial interests or personal relationships that could have appeared to influence the work reported in this paper.

#### Appendix A. Supporting information

Supplementary data associated with this article can be found in the online version at doi:10.1016/j.snb.2021.131231.

#### References

- [1] M.A. Peshkova, T. Sokalski, K.N. Mikhelson, A. Lewenstam, Obtaining Nernstian response of  $\text{Ca}^{2+}$ -selective electrode in a broad concentration range by tuned galvanostatic polarization, *Anal. Chem.* 80 (2008) 9181–9187, <https://doi.org/10.1021/ac8013143>.
- [2] M.A. Peshkova, E.S. Koltashova, G.A. Khripoun, K.N. Mikhelson, Improvement of the ISE Nernstian response by tuned galvanostatic polarization, *Electrochim. Acta* 167 (2015) 187–193, <https://doi.org/10.1016/j.electacta.2015.03.139>.
- [3] E. Hupa, U. Vanamo, J. Bobacka, Novel ion-to-electron transduction principle for solid-contact ISEs, *Electroanalysis* 27 (2015) 591–594, <https://doi.org/10.1002/elan.201400596>.
- [4] U. Vanamo, E. Hupa, V. Yrj ana, J. Bobacka, New signal readout principle for solid-contact ion-selective electrodes, *Anal. Chem.* 88 (2016) 4369–4374, <https://doi.org/10.1021/acs.analchem.5b04800>.
- [5] T. Han, U. Vanamo, J. Bobacka, Influence of electrode geometry on the response of solid-contact ion-selective electrodes when utilizing a new coulometric signal readout method, *ChemElectroChem* 8 (2016) 2071–2077, <https://doi.org/10.1002/celec.201600575>.
- [6] T. Han, U. Mattinen, J. Bobacka, Improving the sensitivity of solid-contact ion-selective electrodes by using coulometric signal transduction, *ACS Sens.* 4 (2019) 900–906, <https://doi.org/10.1021/acssensors.8b01649>.
- [7] T. Han, Z. Mousavi, U. Mattinen, J. Bobacka, Coulometric response characteristics of solid contact ion-selective electrodes for divalent cations, *J. Sol. State Electrochem.* 24 (2020) 2975–2983, <https://doi.org/10.1007/s10008-020-04718-8>.
- [8] T. Han, U. Mattinen, Z. Mousavi, J. Bobacka, Coulometric response of solid-contact anion-sensitive electrodes, *Electrochim. Acta* 367 (2021), 137566, <https://doi.org/10.1016/j.electacta.2020.137566>.
- [9] Z. Jarol mova, T. Han, U. Mattinen, J. Bobacka, E. Bakker, Capacitive model for coulometric readout of ion-selective electrodes, *Anal. Chem.* 90 (2018) 8700–8707, <https://doi.org/10.1021/acs.analchem.8b0214>.
- [10] O. Kondratyeva Ye, E.G. Tolstojatova, D.O. Kirsanov, K.N. Mikhelson, Chronoamperometric and coulometric analysis with ionophore-based ion-selective electrodes: a modified theory and the potassium ion assay in serum samples, *Sens. Actuators B* 310 (2020), 127894, <https://doi.org/10.1016/j.snb.2020.127894>.
- [11] P. Kraikaew, S.K. Sailapu, E. Bakker, Rapid constant potential capacitive measurements with solidcontact ion-selective electrodes coupled to electronic capacitor, *Anal. Chem.* 92 (2020) 14174–14180, <https://doi.org/10.1021/acs.analchem.0c03254>.
- [12] P. Kraikaew, S. Jeanneret, Y. Soda, T. Cherubini, E. Bakker, Ultrasensitive seawater pH measurement by capacitive readout of potentiometric sensors, *ACS Sens.* 5 (2020) 650–654, <https://doi.org/10.1021/acssensors.0c00031>.
- [13] P. Kraikaew, S.K. Sailapu, E. Bakker, Electronic control of constant potential capacitive readout of ion-selective electrodes for high precision sensing, *Sens. Actuators B* 344 (2021), 130282, <https://doi.org/10.1016/j.snb.2021.130282>.
- [14] R.W. Burnett, T.F. Christiansen, A.K. Covington, N. Fogh-Andersen, W. R. K lpmann, A. Lewenstam, A.H.J. Maas, O. M ller-Plathe, C. Sachs, O. Siggaard Andersen, A.L. VanKessel, W.G. Zijlstra, IFCC recommended reference method for the determination of the substance concentration of ionized calcium in undiluted serum, plasma or whole blood, *Clin. Chem. Lab. Med.* 38 (2000) 1301–1314, <https://doi.org/10.1515/CCLM.2000.206>.
- [15] A. Lewenstam, Routines and challenges in clinical application of electrochemical ion-sensors, *Electroanalysis* 26 (2014) 1171–1181, <https://doi.org/10.1002/elan.201400061>.
- [16] G.S. Baird, Ionized calcium, *Clin. Chim. Acta* 412 (2011) 696–701, <https://doi.org/10.1016/j.cca.2011.01.004>.
- [17] J. Bobacka, Potential stability of all-solid-state ion-selective electrodes using conducting polymers as ion-to-electron transducers, *Anal. Chem.* 71 (1999) 4932–4937, <https://doi.org/10.1021/ac990497z>.
- [18] Z. Mousavi, J. Bobacka, A. Ivaska, Potentiometric Ag sensors based on conducting polymers: a comparison between Poly(3,4-ethylenedioxythiophene) and polypyrrole doped with sulfonated calixarenes, *Electroanalysis* 17 (2005) 1609–1615, <https://doi.org/10.1002/elan.200503269>.

- [19] R.-M. Latonen, X. Wang, P. Sjöberg-Eerola, J.-E. Eriksson, M. Bergelin, J. Bobacka, Poly(3,4-ethylenedioxythiophene) based enzyme-electrode configuration for enhanced direct electron transfer type biocatalysis of oxygen reduction, *Electrochim. Acta* 68 (2012) 25–31, <https://doi.org/10.1016/j.electacta.2012.01.107>.
- [20] A. Benoudjit, M.M. Bader, W.W.A.W. Wan Wardatul Amani Wan Salim, Study of electropolymerized PEDOT:PSS transducers for application as electrochemical sensors in aqueous media, *Sens. Bio Sens. Res.* 17 (2018) 18–24, <https://doi.org/10.1016/j.sbsr.2018.01.001>.
- [21] M. Eickenscheidt, E. Singler, T. Stieglitz, Pulsed electropolymerization of PEDOT enabling controlled branching, *Polym. J.* 51 (2019) 1029–1036, <https://doi.org/10.1038/s41428-019-0213-4>.
- [22] Y. Seki, M. Takahashi, M. Takashiri, Effects of different electrolytes and film thicknesses on structural and thermoelectric properties of electropolymerized poly(3,4-ethylenedioxythiophene) films, *RSC Adv.* 9 (2019) 15957–15965, <https://doi.org/10.1039/c9ra02310k>.
- [23] K.N. Mikhelson, *Ion-selective Electrodes (Lecture Notes in Chemistry, Vol. 81)*, Springer, Heidelberg-New York-Dordrecht-London, 2013, <https://doi.org/10.1007/978-3-642-36886-8>.
- [24] N. Jassam, S. Gopaul, P. McShane, A. McHugh, R. Coleman, D. Thompson, J. H. Barth, Calcium adjustment equations in neonates and children, *Ann. Clin. Biochem.* 49 (2012) 352–358, <https://doi.org/10.1258/acb.2011.011060>.
- [25] P. Ridefelt, J. Helmersson-Karlqvist, Albumin adjustment of total calcium does not improve the estimation of calcium status, *Scand. J. Clin. Lab. Investig.* 77 (2017) 442–447, <https://doi.org/10.1080/00365513.2017.1336568>.
- [26] I.A. Lian, A. Åsberg, Should total calcium be adjusted for albumin? A retrospective observational study of laboratory data from central Norway, *BMJ Open* 8 (2018) 1–7, <https://doi.org/10.1136/bmjopen-2017-017703>.
- [27] C.M. Kenny, C.E. Murphy, D.S. Boyce, D.M. Ashley, J. Jahanmir, Things we do for no reason calculating a “corrected calcium” level, *J. Hosp. Med.* 16 (2021) 499–501, <https://doi.org/10.12788/jhm.3619>.
- [28] D.A. Bushinsky, R.D. Monk, Electrolyte quintet: calcium, *Lancet* 352 (1998) 306–311, [https://doi.org/10.1016/s0140-6736\(97\)12331-5](https://doi.org/10.1016/s0140-6736(97)12331-5).
- [29] A.A. Mir, B. Goyal, S.K. Datta, S. Ikkurthi, A. Pal, Comparison between measured and calculated free calcium values at different serum albumin concentrations, *J. Lab. Phys.* 8 (2016) 71–76, <https://doi.org/10.4103/0974-2727.180785>.
- [30] M. Morishita, Y. Maruyama, M. Nakao, N. Matsuo, Y. Tanno, I. Ohkido, M. Ikeda, T. Yokoo, Factors affecting the relationship between ionized and corrected calcium levels in peritoneal dialysis patients: a retrospective cross-sectional study, *BMC Nephrol.* 21 (2020) 370, <https://doi.org/10.1186/s12882-020-02033-y>.
- [31] L. Jafri, A.H. Khan, S. Azeem, Ionized calcium measurement in serum and plasma by ion selective electrodes: comparison of measured and calculated parameters, *Ind. J. Clin. Biochem.* 29 (2014) 327–332, <https://doi.org/10.1007/s12291-013-0360-x>.
- [32] A. Besarab, A. Deguzman, J.W. Swanson, Effect of albumin and free calcium concentrations on calcium binding in vitro, *J. Clin. Pathol.* 34 (1981) 1361–1367, <https://doi.org/10.1136/jcp.34.12.1361>.
- [33] U. Kragh-Hansen, H. Vorum, Quantitative analyses of the interaction between calcium ions and human serum albumin, *Clin. Chem.* 39 (1993) 202–208, <https://doi.org/10.1093/clinchem/39.2.202>.
- [34] H. Vorum, K. Fisker, M. Otagiri, A.O. Pedersen, U. Kragh-Hansen, Calcium ion binding to clinically relevant chemical modifications of human serum albumin, *Clin. Chem.* 41 (1996) 1654–1661, <https://doi.org/10.1093/clinchem/41.11.1654>.

**Anna V. Bondar** is graduating student in the St.Petersburg State University. She is working on ionophore-based electrochemical sensors.

**Valentina M. Keresten** is master student in the St.Petersburg State University. She is working on ionophore-based electrochemical sensors.

**Konstantin N. Mikhelson** graduated from the Leningrad State University (Ms.Sc.) in 1975. He received his Ph.D. in physical chemistry (1982) from the Leningrad State University and Dr.Sc. in electrochemistry (2003) from the St.Petersburg State University. His research interests refer to chemical sensors, in particular to electrochemical and optical sensors based on ionophores, to computer simulations of the sensor response, and to the electrochemistry of liquid/liquid interfaces.